ELECTROMECHANICAL INDUCTORS FOR POWER CONVERTER APPLICATIONS

Yaxing Zhang*, David P. Arnold
Interdisciplinary Microsystems Group, Dept. Electrical and Computer Engineering, University of Florida, Gainesville, FL, United States
*Presenting Author: yashin@ufl.edu

Abstract: This paper presents the concept, theory, and demonstration of electromechanical inductors that couple an electrical conductor with a mechanical energy storage component in order to boost the electrical inductance over a specific frequency band. Measurements of mesoscale prototypes indicate an inductance boost >10,000x compared to static electrical devices. The results here are a step toward ultra-high-inductance-density microfabricated devices intended to dramatically reduce the size and mass of switched-mode power supplies.

Keywords: inductor, electrodynamic transduction, power converter, switched-mode power supply

INTRODUCTION

Inductors and transformers are foundational elements for power electronic circuits such as DC-DC converters, filters and etc. These elements rely on magnetic fields for inductive energy storage or energy transfer. In practice, these components are often physically bulky and hard to integrate compared to the other circuit components. Since the power system size and performance often constrains the overall functionality and endurance of a battery powered device, much research has recently focused on miniaturizing these components. One major thrust is microfabricated inductors to enable fully integrated, single-chip power converters [1-7], but it remains theoretically and technologically challenging to realize high-inductance-density, high-efficiency inductors in chip-scale form factors.

The traditional approach of increasing the inductance of on-chip inductor is to incorporate a soft magnetic core. Gardner et al. have employed Co-Zr-Ta magnetic material to obtain on-chip inductance density up to 1.7 $\mu H/mm^2$ with quality factor up to 8 around 40 MHz [6]. The performance is limited by magnetic saturation and magnetic losses associated with the soft magnet material, especially at high frequencies. Air-core on-chip inductor can be used in this frequency range while trading efficiency with inductance density. Meyer et al. demonstrated air-core inductors with inductance densities of up to 100 nH/mm^2 and quality factors around 20 in the frequency range from 100 MHz to 500 MHz [7]. However, for use in a functional power converter, the switching losses from conventional semiconductor devices operated in this frequency range are quite high, presenting significant circuit design challenges for achieving high power converter efficiency.

As an alternative approach, mechanical and electromechanical devices have been investigated for use in electrical power converters. To avoid the use of on-chip inductors, microelectromechanical power converters [8-10] have been reported to achieve dc voltage conversion with the help of mechanical energy storage. These devices were operated in charge pump circuits with electrostatic actuation control on variable capacitors that are mechanically coupled. These types of converters are limited to high output voltage and low output power because of the large output impedance [9]. Low efficiency is also reported due to the external power loss from electrostatic actuation control. The challenging regulation scheme associated with the switched-capacitor power converter further hinders the usage of this type of converter.

This paper proposes an alternative strategy of directly using mechanical energy storage in the application of power converter circuitry. The use of mechanical elements to achieve circuit functionality is well known in the area of MEMS-based resonators [11]. Additionally, mechanical energy storage can be very energy-dense as reported recently [12]. It is also known that with appropriate electromechanical transduction schemes, mechanical components can function as electrical components in circuit. For example, a mechanical spring can "appear" as an electrical inductor through electrodynamic transduction [13]. The key idea in this paper is to increase the apparent electrical inductance of a standard inductor by storing additional energy through electrodynamic coupling to a mechanical flexure. The resulting device is coined as an "electromechanical inductor."

DEVICE STRUCTURES

Electrodynamic transduction relies on the relative motion between a magnet and a conductor. In the presence of an external magnetic field, current flowing through a metal wire will force the movement of either the wire or the magnet, depending on the mechanical boundary conditions. Therefore, candidate electro-mechanical inductor structures can be grouped into two categories: moving-magnet and moving-conductor. Two prototype structures are illustrated in Fig.1 for investigation: (a) cantilever-supported moving magnet above a fixed, planar coil and (b) clamped-clamped moving wire above a fixed magnet.

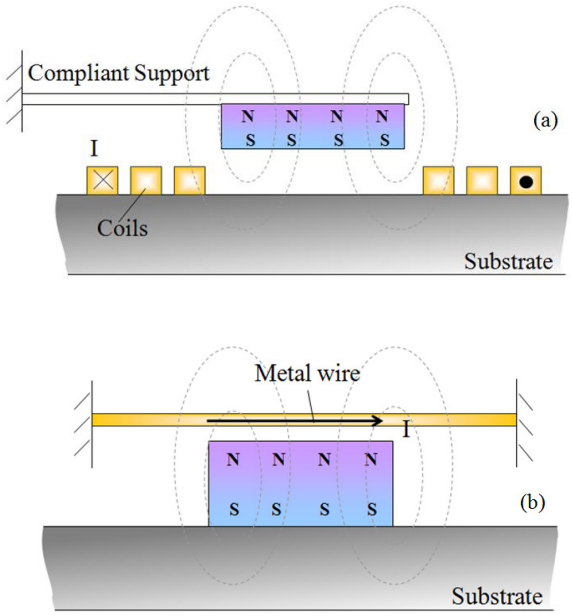

Fig. 1: Candidate electromechanical inductor structures.

For the moving-magnet case shown in Fig.1 (a), the mechanical and electrical elements are separate from each other. Current flowing through the fixed electrical coil will generate a magnetic field as modeled by conventional electrical inductor. In addition, the current will enact a force on the magnet and excite the motion of the attached mechanical system, which in turn generates an electromotive force (induction voltage) across the terminals of the electrical coil. Energy is thereby transferred between the electrical domain and mechanical domain. For the moving conductor case shown in Fig.1 (b), a similar energy transfer mechanism applies. In this case, the magnet is static, and the force will cause a transverse oscillation of the wire.

DEVICE MODEL

The physical phenomenon can be modeled with an equivalent lumped-element circuit (Fig.2) that captures the coupled electromechanical physics [13]. R_e, L_e represent the electrical resistance and inductance while b_m, $C_m = 1/k_m$, and m_m correspond to the lumped damping factor, compliance (inverse of stiffness) and inertance of the mechanical structure. Electrodynamic coupling is modeled by a gyrator connecting the two energy domains.

The electromechanical transduction can be described by the following simplified linear equations, specifying the relationship between voltage V and current i in the electrical domain and force F and velocity u in the mechanical domain [13]:

$$F = Ki, \quad (1)$$

$$V = Ku. \quad (2)$$

The electrodynamic transduction coefficient K is defined as the product of the conductor length l and the average magnetic flux density B perpendicular to the structure motion.

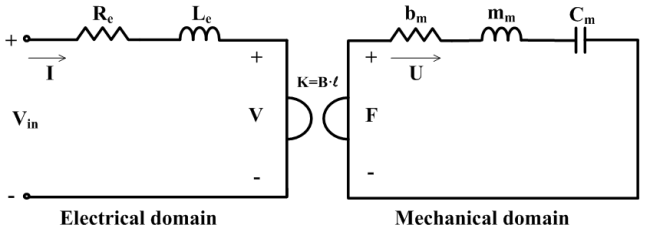

Fig. 2: Lumped-element model for electromechanical inductor.

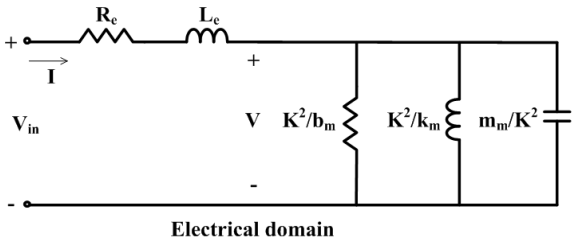

Fig. 3: Equivalent electrical model for electro-mechanical inductor.

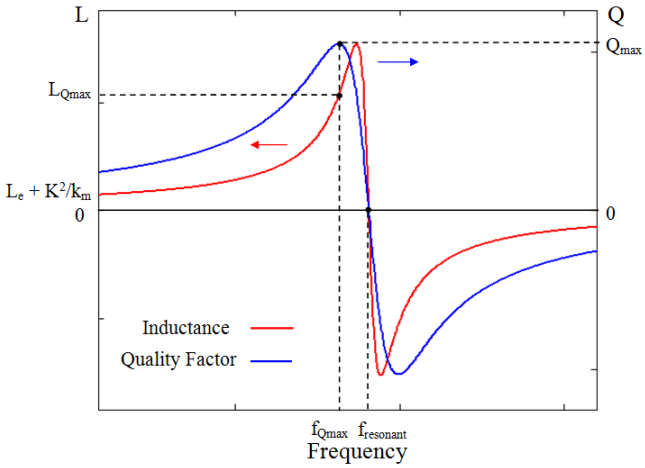

Fig. 4: Example curves of apparent inductance and quality factor versus frequency for electromechanical inductor.

Fig.3 shows the equivalent electrical model after impedance transformation across the gyrator. The mechanical components "appear" as a parallel-connected RLC tank in series with the electrical resistance and inductance. The apparent inductance, arising from the structure compliance, is K^2/k_m. The apparent capacitance m_m/K^2 arises from the mechanical mass, and an additional resistance K^2/b_m arises from the mechanical damping. These equivalent lumped circuit parameters can be designed to meet different specifications by appropriate selection of materials and structural dimensions.

Compared with a conventional electrical inductor, the electromechanical structure shows an inductance boost due to the presence of the energy-storing mechanical compliance. Fig. 4 shows an example curve for the apparent inductance and the quality factor versus frequency. A highly underdamped mechanical system and a small electrical inductance are assumed here.

When the exciting sinusoidal frequency is much lower than the resonant frequency of the mechanical resonator, the total apparent inductance is the sum of the electrical inductance L_e and the apparent inductance K^2/k_m from the mechanical compliance. As the operating frequency approaches the mechanical resonance, the apparent inductance and resistance both increase. At a particular frequency (denoted as f_{Qmax} in Fig.4), a maximum quality factor is reached. To function as an inductor in a switching power supply, this might be one of the desired operating frequencies. When the exciting frequency is further increased, a maximum apparent inductance is reached. Just beyond this frequency, the electromechanical system resonance occurs, and the network appears purely dissipative (zero reactance). As the frequency keeps increasing, the electromechanical network will first show a capacitive reactance (denoted as negative apparent inductance in Fig.4), and then trend toward inductive characteristics as the frequency continues higher. At frequencies much higher than the mechanical resonance, the system appears as a conventional electrical inductor. Note that Fig.4 only includes the narrow frequency range around the resonance for the purpose of clarifying the electromechanical interaction.

EXPERIMENTAL RESULTS

Mesoscale structures are built (Fig.5) and tested to demonstrate the concepts. Different mechanical structure dimensions, electrical conductor dimensions, and magnetic fields are chosen to study the effect of these design variables on the performance of the prototypes. Detailed results are summarized in Tables 1 and 2 for four moving-magnet and five moving-conductor prototypes.

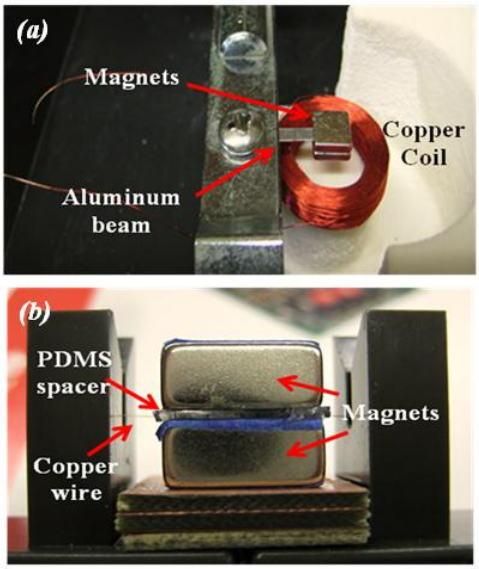

Fig. 5: Mesoscale prototypes (a) moving-magnet and (b) moving-conductor

Fig.6 shows the measured apparent electrical inductance and quality factor versus frequency for a moving-magnet and a moving-conductor case. Dotted lines are fitted curves based on the model shown in Fig.2. Moving-magnet Device 1 shows a maximum Q of 1.3 with inductance of 260 mH at 82.4 Hz, a 22x improvement over its electrical inductance. Similarly, moving-conductor Device 5 yields a maximum Q of 7.3 with inductance of 135 µH at 696 Hz, a 13500x improvement over the electrical inductance. Note here that the moving-magnet device exhibits higher inductance, but lower Q in comparison to the moving-conductor device.

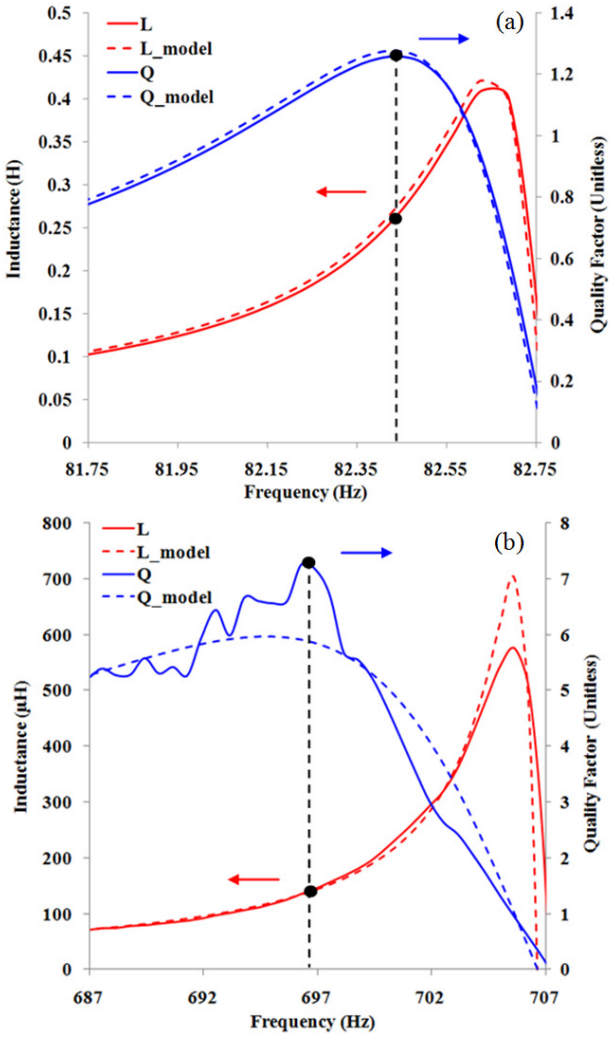

Fig. 6: Electromechanical inductor measurement results (a) moving-magnet Device 1 and (b) moving-conductor Device 5.

Table 1 summarizes the different moving-magnet prototypes. Comparing Devices 1 and 2, the larger conductor volume contributes to a boost in quality factor and apparent inductance. By comparing Devices 2 and 4, the longer and narrower cantilever beam is shown to yield a larger quality factor and a larger inductance (L_{Qmax}).

Table 2 summarizes the different moving-conductor prototypes. Compared with the moving-magnet devices, the moving-conductor devices have a much smaller conductor volume, which results in a decrease of the resonating inductance. However, the

lower electrical resistance and lower mechanical damping results in higher quality factors. Device 5 vs. 6 and Device 7 vs. 8 show the importance of a large magnetic field, while Device 5 and Device 7 (using different types of wires) illustrate the trade-off between Q and resonating inductance. Comparison between Devices 8 and 9 also confirms the merit of having a longer, more compliant flexure.

Table 1: Performance summary for the moving-magnet prototypes

Device	1	2	3	4
Conductor	Cu	Cu	Cu	Cu
Mechanical Flexure	Al	Al	Al	Al
Conductor Volume (mm^3)	907.13	450.62	450.62	450.62
Flexure Dimension (mm)	12 ×2.2 ×0.2	12 ×2.2 ×0.2	17 ×2.2 ×0.2	17 ×9 ×0.2
B-field (T)	0.02	0.03	0.03	0.03
f_{Qmax} (Hz)	82.44	133.47	61.40	102.45
Q_{max}	1.3	1.1	1.8	0.6
L_{Qmax} (μH)	260000	66819	282902	48481
L_e (μH)	11875	4559	4559	4559
L Boost	22	15	62	11

Table 2: Performance summary for the moving-conductor prototypes

Device	5	6	7	8	9
Conductor	Cu	Cu	Al	Al	Al
Mechanical Flexure	Cu	Cu	Al	Al	Al
Conductor Volume (mm^3)	0.27	0.27	0.01	0.01	0.04
Flexure Dimension (mm)*	24 ×0.09	24 ×0.09	24 ×0.025	24 ×0.025	84 ×0.025
B-field (T)	0.28	0.07	0.28	0.07	0.26
f_{Qmax} (Hz)	696.25	606.88	1926.25	3152.62	59.55
Q_{max}	7.3	0.8	2.5	0.7	1.7
L_{Qmax} (μH)	135	15	532	63	3203
L_e (μH)	0.01	0.01	0.02	0.02	0.2
L Boost	13500	1500	26600	3150	16015

* Conductor length × diameter of the circular cross-section

CONCLUSION

In this paper, the idea of electromechanical inductors is proposed as alternative solution for ultra-high-inductance-density microfabricated devices. The concept involves electrodynamically coupling an electrical conductor with a mechanical energy storage component in order to obtain a drastic boost of the electrical inductance over a specific frequency range. Mesoscale prototype structures are built and tested. The results show an inductance boost >10,000x compared to the electrical inductance.

The quality factors of the preliminary test results are still somewhat low for utility in power electronics application. However, quality factor is expected to improve with careful design of the magnet field pattern and mechanical flexure. Vacuum operation is another option to increase the quality factor by lowering the mechanical damping coefficient. Eventually, microfabricated structures with micromagnets [14] can be anticipated to have higher mechanical quality factor and higher operating frequencies, enabling a better fit into existing power electronic circuits.

ACKNOWLEDGEMENTS

This work is supported by DARPA grant N66001-09-1-2095.

REFERENCES

[1] Onizuka K, Inagaki K, Kawaguchi H, Takamiya M, Sakurai T 2007 Stacked-Chip Implementation of On-Chip Buck Converter for Distributed Power Supply System in SiPs IEEE J. Solid-State Circuits **42** 2404-10

[2] Wens M and Steyaert M 2008 A Fully-Integrated 130nm CMOS DC-DC Step-Down Converter, Regulated by a Constant On/Off-Time Control System the ESSCIRC 2008 62-5

[3] Wibben J and Harjani R 2008 A High-Efficiency DC-DC Converter Using 2nH Integrated Inductors IEEE J. Solid-State Circuits, **43**, 844-54

[4] Meere R, O'Donnell T, Bergveld H J, Wang N, O'Mathuna S C 2009 Analysis of Microinductor Performance in a 20-100 MHz DC/DC Converter IEEE Trans. Power Electron. **24** 2212-8

[5] Ni J, Hong Z, Liu B Y 2009 Improved on-chip components for integrated DC-DC converters in 0.13 μm CMOS ESSCIRC 2009 448-51

[6] Gardner D S, Schrom G, Paillet F, Jamieson B, Karnik T, Borkar S 2009 Review of On-Chip Inductor Structures With Magnetic Films IEEE Trans. Magn. **45** 4760-6

[7] Meyer C D, Bedair S S, Morgan B C, Arnold D P 2010 High-Inductance-Density, Air-Core, Power Inductors, and Transformers Designed for Operation at 100–500 MHz IEEE Trans. Magn. **46** 2236-9

[8] Noworolski J M and Sanders S R 1992 An electrostatic microresonant power conversion device Power Electronics Specialists Conf. 1992, PESC '92 Record., 23rd IEEE Ann.Conf.

[9] Haas C H and Kraft M 2004 Modelling and analysis of a MEMS approach to dc voltage step-up conversion J. Micromech. Microeng. **14** S114

[10] Hill M and Mahony C O 2006 Modelling and performance evaluation of a MEMS dc/dc converter J. Micromech. Microeng. **16** S149

[11] Nguyen C T C 2007 MEMS technology for timing and frequency control IEEE Trans. Ultrasonics, Ferroelectrics and Frequency Control, **54** 251-70

[12] Hill F, Havel T, Hart A J, Livermore C 2008 Storing Elastic Energy in Carbon Nanotubes PowerMEMS 2008 (Sendai, Japan, 9-12 November 2008) 35–38

[13] Cheng S, Wang N, Arnold D P 2007 Modeling of magnetic vibrational energy harvesters using equivalent circuit representations J. Micromech. Microeng. **17** S2328

[14] Arnold D P and Wang N 2009 Permanent Magnets for MEMS J. Micromech. Microeng. **18** S1255